Triggered Release of Aqueous Content from Liposome-Derived Sol−Gel Nanocapsules

Yael Steinberg,[†] Avi Schroeder,[‡,§] Yeshayahu Talmon,[||] Judith Schmidt,[||] Rafail L. Khalfin,[||] Yachin Cohen,[||] Jean-Marie Devoisselle,[⊥] Sylvie Begu,[⊥] and David Avnir*[,†]

Institute of Chemistry, The Hebrew University of Jerusalem, Jerusalem 91904, Israel, Laboratory of Liposome and Membrane Research, Department of Biochemistry, The Hebrew University-Hadassah Medical School, Jerusalem 91120, Israel, Department of Chemical Engineering, Ben-Gurion University of the Negev, Beer Sheva 84105, Israel, Department of Chemical Engineering, Technion-Israel Institute of Technology, Haifa 32000, Israel, and UMR CNRS/ENSCM/UM2/UM1 5253, Institut C. Gerhardt, UFR des Sciences Pharmaceutiques et Biologiques, 15 avenue Charles Flahault, 34293 Montpellier cedex 05, France

Received July 31, 2007. In Final Form: September 16, 2007

Liposomes prepared from a mixture of L-α-dipalmitoylphosphatidylcholine and the PEGilated phospholipid *N*-(carbonylmethoxypoly(ethylene glycol 2000))-1,2-distearoyl-*sn*-glycero-3-phosphoethanolamine were used as templates for the production of silica and alkylated silica ∼100 nm capsules, "liposils", entrapping aqueous solutions of anionic dyes. Triggered release of this content was successfully affected by either low-frequency ultrasound or by microwave treatments. Cryo-TEM was used to follow the formation process of these particles, which are aggregated in a chain-like manner. A mechanism explaining this phenomenon is suggested.

1. Introduction

We report the microwave (MW) or ultrasound (US) triggered release of aqueous content from rigid ceramic submicron hollow silica spheres. The bursting of a capsule by using an external signal has considerable potential applications, wherever remote activation of content-release is needed. This concept has been demonstrated for polymeric capsules[1−8] and for soft liposomes[9] and micelles,[10] leaving the idea of external triggered release from rigid ceramic capsules relatively unexplored. Noteworthy work in this field is that of Sun et al.,[11] who photolyzed a single ceramic capsule. The particles we have selected for this study are ∼100 nm silica shells, ∼10 nm thick, synthesized around liposomes (which apparently remain intact within the shell). This system was originally developed by Begu et al.,[12,13] who aptly termed these particles "liposils". We were motivated to use these particles because, while methods for formation of silica capsules are well-known[14−16] and inclusion of an oily core within silica shells is commercialized,[17] practical approaches for the inclusion of water solutions in such particles are still in their infancy. In this context, Begu et al. reported that the particles do not leak but release their contents above 260 °C.[13]

We have advanced that original report in a number of ways: First, we were able to reduce the cluster-like particle aggregation—an outcome of the original procedure—into chain-like aggregates of particles, by the use of PEGilated phoshpholipids, which are at the focus of this report. It should be noted that chain-like aggregated spheres are quite rare; we regard their formation as an unexpected result of this study, which is of general interest.[18] Second, we extended the liposil's shell nature to include hydrophobic modifications. Third, we showed the feasibility of the triggered release of the encapsulated content with two types of remote energy sources. And fourth, we have explored the stages of the formation of these particles using cryo-TEM microscopy.

We recall that aqueous systems can be dielectrically heated by MW radiation,[19] and this source of energy has indeed been used for release purposes. A representative example for MW-triggered release from liposomes is the report of Liburdy and Magin,[20] who suggested a mechanism of increase in the bilayer permeability. In yet another representative example, Miyazaki et al. demonstrated likewise a higher rate of release of 5-fluorouracil from an ethylenevinyl alcohol copolymer matrix,

* Corresponding author. E-mail: david@chem.huji.ac.il.
[†] The Hebrew University of Jerusalem.
[‡] The Hebrew University-Hadassah Medical School.
[§] Ben-Gurion University of the Negev.
[||] Technion-Israel Institute of Technology.
[⊥] Institut C. Gerhardt.

(1) Lu, Z.; Prouty, M. D.; Guo, Z.; Golub, V. O.; Kumar, C. S. S. R.; Lvov, Y. M. *Langmuir* **2005**, *21*, 2042−2050.
(2) Shchukin, D. G.; Gorin, D. A.; Mohwald, H. *Langmuir* **2006**, *22*, 7400−7404.
(3) Skirtach, A. G.; De Geest, B. G.; Mamedov, A.; Antipov, A. A.; Kotov, N. A.; Sukhorukov, G. B. *J. Mater. Chem.* **2007**, *17*, 1050−1054.
(4) Unger, E. C.; Hersh, E.; Vannan, M.; McCreery, T. *Echocardiography* **2001**, *18*, 355−361.
(5) Skirtach, A. G.; Antipov, A. A.; Shchukin, D. G.; Sukhorukov, G. B. *Langmuir* **2004**, *20*, 6988−6992.
(6) Radt, B.; Smith, T. A.; Caruso, F. *Adv. Mater.* **2002**, *16*, 2184−2189.
(7) Radziuk, D.; Shchukin, D. G.; Skirtach, A.; Mohwald, H.; Sukhorukov, G. *Langmuir* **2007**, *23*, 4612−4617.
(8) Mathiowitz, E.; Cohen, M. D. *J. Membr. Sci.* **1989**, *40*, 67−86.
(9) Schroeder, A.; Avnir, Y.; Weisman, S.; Tzemach, D.; Najajreh, Y.; Gabizon, A.; Talmon, Y.; Kost, J.; Barenholz, Y. *Langmuir* **2007**, *23*, 4019−4025.
(10) Husseini, G. A.; Myrup, G. D.; Pitt, W. G.; Christensen, D. A.; Rapoport, N. Y. *J. Controlled Release* **2000**, *69*, 43−52.
(11) Sun, B.; Mutch, S. A.; Lorenz, R. M.; Chiu, D. T. *Langmuir* **2005**, *21*, 10763−10769.
(12) Begu, S.; Durand, R.; Lerner, D. A.; Charnay, C.; Tourne-Peteilh, C.; Devoisselle, J. M. *Chem. Commun.* **2003**, (5), 640−641.
(13) Begu, S.; Girod, S.; Lerner, D. A.; Jardiller, N.; Tourne-Peteilh, C.; Devoisselle, J. M. *J. Mater. Chem.* **2004**, *14*, 1316−1320.
(14) Li, L.; Yokoyama, H. *Angew. Chem. Int. Ed.* **2006**, *45*, 6338−6341.
(15) Hashizume, M.; Inoue, H.; Katagiri, K.; Ikeda, A.; Kikuchi, J. *J. Sol−Gel Sci. Technol.* **2004**, *31*, 99−102.
(16) Matsui, K.; Sando, S.; Sera, T.; Aoyama, Y.; Sasaki, Y.; Komatsu, T.; Terashima, T.; Kikuchi, J. *J. Am. Chem. Soc.* **2006**, *128*, 3114−3115.
(17) Lapidot, N.; Gans, O.; Biagini, F.; Sosonkin, L.; Rottman, C. *J. Sol−Gel Sci. Technol.* **2003**, *26*, 67−72.
(18) Tang, Z.; Kotov, N. A. *Adv. Mater.* **2005**, *17*, 951−962.
(19) Michael, D.; Mingos, P.; Baghurst, D. R. *Chem. Soc. Rev.* **1991**, *20*, 1−47.
(20) Liburdy, R. P.; Magin, R. L. *Radiat. Res.* **1985**, *103*, 266−275.

10.1021/la702311f CCC: $37.00
Published on Web 10/23/2007

induced by MW.[21] Lately the effect of MW radiation on polymer microcapsules containing inorganic nanoparticles has also been studied.[22] US—a different source of energy—refers to sound waves with frequencies above 20 kHz, the audible limit of the human ear. Unlike electromagnetic microwaves, US is completely mechanical in nature and involves pressure waves that run through the environment surrounding the source.[23] US has been used to increase the permeability of liposomes, thus enabling controlled drug release.[9] The effect was found to be connected with cavitation, which is the formation, growth, and implosive collapse of bubbles in a liquid. US was also shown to facilitate content release by causing enhanced erosion of polymeric matrices or enhanced diffusion out of such matrices[24] and by rupturing the shells of polymeric microcapsules.[2,3,4] To the best of our knowledge, the response of aqueous core/ceramic shell particles to US or MW radiation was not explored.

2. Experimental Details

Chemicals. Tetraethylorthosilicate (TEOS, 98%), allyltrimethoxysilane (ATMS, 95%), octadecyltrimethoxysilane (OTMS, 90%), Congo Red (CR, 97%), and Safranin O (SaO, 99%) were from Aldrich. Methylene Blue (MB) was from Merck. Phenylbenzimidazole sulfonic acid (PSA, known commercially as Neo Heliopan Hydro) was from Symrise. L-α-Dipalmitoylphosphatidylcholine (DPPC) was from Lipoid. *N*-(Carbonylmethoxypoly(ethylene glycol 2000))-1,2-distearoyl-*sn*-glycero-3-phosphoethanolamine (mPEG^{2000}-DSPE, MW 2774) was from Genzyme (Switzrland).

Buffer Preparation. Na_2HPO_4 (1.78 g) was dissolved in 1.0 L of triply distilled water (TDW). The pH was adjusted to 7.4 by adding HCl and NaOH as necessary. The solution was filtered with a 0.2 μm pore size membrane.

Preparation of the Liposomes. DPPC liposomes were prepared as described in ref 13. DPPC/mPEG^{2000}-DSPE liposomes were prepared as described in ref 9 with 99.2 mol % DPPC and 0.8 mol % mPEG^{2000}-DSPE. The phospholipids were dissolved in absolute ethanol at 50 °C (above the lipid phase transition temperature, T_m, of DPPC, 41 °C) and added to the buffer solution described above to yield a 10 mg mL^{-1} suspension. The initial amount of ethanol was 10 vol % of the solution. The resulting multilamellar vesicles were downsized to form small unilamellar vesicles by the same stepwise extrusion as for the DPPC liposomes.

Liposils Preparation. The silica shell was formed by a method similar to that described in ref 13, for both the DPPC liposomes (liposils) and for the MPEG-DSPE/DPPC liposomes (PEG-liposils). TEOS (535 μL, 0.50 g) was transferred to a plastic vial, and 40.0 mL of the buffer solution and 3.0 mL of the liposome suspension were added. The vials were covered and stirred gently at 130 rpm using a small magnetic stirrer. After 48 h of stirring at room temperature, 5.0 mg of NaF was added, and the stirring continued for an additional 24-h period. The resulting particles were rinsed several times with TDW using a centrifuge at a speed of 3400−4200 rpm, for 5 min each time.

Encapsulation within the PEG-Liposils. All encapsulation experiments were carried out with PEG-liposils. The dye used for rupture experiments was CR. Two other dyes and one UV-sunscreen were also tested for encapsulation: MB, SaO, and PSA. They will be referred to as dyes from this point on. Different concentrations of dye were dissolved in the phosphate buffer (CR, MB, and SaO, 5.0×10^{-4} M; PSA, 7.5×10^{-4} M), after which the dye-filled liposomes were prepared and used for PEG-liposil preparation. Colorless buffer was used as the dilution medium. For the purpose of dye release experiments, the samples were washed with TDW by centrifugation until the liquid appeared colorless and were concentrated 4-fold.

Variation of the Silica Shell Composition. CR-containing PEG-liposils were also synthesized with part of the TEOS substituted for each of the two chosen monomers ATMS and OTMS at molar ratios of 5, 10, and 20%. The rest of the synthesis was performed as described above. Additionally, three samples were prepared with reduced amounts of TEOS, 0.75, 0.50, and 0.33 of the original amount.

Ultrasonication. The parameters that can be screened when using the low-frequency US probe are intensity and time. Frequency was set at 20 kHz (see instrument details below) with a full duty cycle. During the experiment, the probe was dipped into the sample solution, which was in turn immersed in a water bath. The bath regulates the sample temperature so that there is no considerable heating of the sample or loss of vapor. Each sample that was exposed to US contained 3.0 mL of PEG-liposils solution. After exposure to US, the samples were centrifuged for 30 min at 5400 rpm, and the supernatant's absorbance at 497 nm, CR's maximum, was measured by spectrophotometer. In order to test the effect of ultrasonication time and intensity, two sets of experiments were performed. In each set, either the time or intensity was kept constant while the other parameter was changed from sample to sample. The parameters used were time = 120 s, with varying intensity, or intensity = 5.0 W/cm^2, with varying time. For another sample, a statistical analysis was performed on HR-SEM images of PEG-liposils loaded with CR from a set of varying intensity US experiments at 120 s, using an enlargement of ×100 000. The number of damaged particles was counted and averaged over at least eight frames and the total number of particles per frame was averaged over three frames for each sample. Any particle with a visible flaw was considered damaged.

Microwave Heating. MW heating experiments were performed as follows: A vial was weighed and 5.0 mL of the sample was weighed into it. The solution was transferred into a small, elongated flask in order to reduce the quantity of liquid lost through splashing during MW heating. After heating, the remaining liquid was transferred into a clean preweighed vial. The weight of evaporated water was calculated and TDW was added to the sample to compensate for the loss. The sample was centrifuged for 10 min at 3600 rpm and the supernatant's absorbance at 497 nm was measured. Some of the samples were viewed by HR-SEM. The parameter that was tested was variation of boiling time: The heating program was set to reach boiling temperature within 30 s and then to continue the heating at this temperature for increasingly longer times. The maximal power input was set to 1000 W. Another set of experiments was performed on batches of PEG-liposils with different shell compositions. The tested samples included the 5, 10, and 20% ATMS and OTMS particles and the PEG-liposils with reduced amounts of TEOS. They were all allowed 30 s to reach boiling temperature at 1000 W maximum power input.

Blanks and Repetitions. For a single batch, five repetitions of the rupture experiments were made on five samples of the same batch. For the different batches, a single rupture experiment was performed on each batch, five experiments in total, and the maximal deviation from the average was taken as the error estimate for subsequent experiments. The absorbance of a clean sample that had not undergone exposure to MW or US was used as the benchmark to which absorbance of exposed samples was compared. The absorbance of this blank sample was subtracted from the values of the exposed samples, so the reported concentration of CR in exposed samples reflects the actual change in CR concentration. In the case of exposure to US, an extra blank experiment was necessary. After undergoing ultrasonication, all exposed samples contained fine particles that remained suspended in the solution to some extent even after prolonged, fast centrifugation. It was necessary to test the effect of this suspension on absorbance, as turbidity is known to influence absorbance spectra. For this purpose a colorless sample underwent an US experiment identical to the one performed on the colored sample. These two samples were subjected to US at increasing power. The colorless sample showed no significant change in the absorbance spectra with power input; that assured that the different

(21) Miyazaki, S.; Yokouchi, C.; Takada, M. *Chem. Pharm. Bull.* **1989**, *37*, 208−210.
(22) Gorin, D. A.; Shchukin, D. G.; Mikhailov, A. I.; Kohler, K.; Sergeev, S. A.; Portnov, S. A.; Taranov, I. V.; Kislov, V. V.; Sukhorukov, G. B. *Technol. Phys. Lett.* **2006**, *32*, 70−72.
(23) Ng, K. Y.; Liu, Y. *Med. Res. Rev.* **2002**, *22*, 204−223.
(24) Kost, J.; Langer, R. *Adv. Drug Delivery Rev.* **2001**, *46*, 125−148.

absorbance values of each colored sample were a result of color release, not of turbidity effects.

Instrumentation. *Transmission electron microscopy* (TEM) was carried out with an FEI Tecnai 12 equipped with a SIS MegaView II CCD camera and operated at 100 kV. Samples were prepared by depositing the particle suspension on a 300 mesh copper grid covered with Formvar and carbon. *Scanning electron microscopy* was performed on an FEI Sirion high-resolution SEM (HR-SEM) operated at 3 or 5 kV. A drop of the particle suspension was placed on a glass disk stuck onto a metal stub, a strip of carbon tape was stretched from the glass surface to the stub, and the air-dried sample was coated with gold. *The cryo-TEM* observations were carried out on an FEI Tecnai T12 G^2 TEM equipped with a Gatan US1000 high-resolution camera and a Gata 626 cooling holder system. Specimen preparation is described by Danino et al.[25] *ζ-Potential measurements* were carried out with a Malvern ZEN3600 NanoSizer. Concentrations of the released dye were determined *spectrophotometrically* using a Hewlett-Packard 8452A diode-array UV−vis spectrophotometer. *Ultrasonic treatment* was carried out with a Sonics & Materials VC400 20 kHz low-frequency ultrasonic processor. *Microwave heating* was carried out with a Milestone MicroSYNTH laboratory oven. *Extrusions* were performed using an Avanti Polar Lipids Mini Extruder and a Northern Lipids Lipex extruder, with Osmonics Poretics and Whatman Nuclepore polycarbonate membranes. *Small-angle X-ray scattering (SAXS*) was performed using a small-angle diffractometer (Bruker Nanostar, KFF CU 2 K-90) with Cu Kα radiation from a sealed tube, two Göbel mirrors, and two-pinhole collimation that results in a beam 300 mm in diameter on the sample. The scattering patterns were recorded for 18 h (generator powered at 40 kV and 20 mA) by a 10 × 10 cm^2 two-dimensional position-sensitive wire detector that is positioned 65 cm behind the sample. The scattered intensity $I(h)$ was recorded in the interval $0.12 < h < 3.2$ nm^{-1}, where h is the scattering vector defined as $h = (4\pi/\lambda)\sin(\theta)$, 2θ is the scattering angle, and λ is the radiation wavelength (0.1542 nm). The aqueous dispersion under study was sealed in a thin-walled capillary (glass) of about 2 mm diameter and 0.01 mm wall thickness, sealed with epoxy glue, and measured under vacuum at ambient temperature. Measurements were taken from two parts of the capillary, a transparent portion and a nontransparent part, due to material precipitation. Only the latter was analyzed, as the signal from the former was weak. $I(h)$ was normalized to the following parameters: time, solid angle, primary beam intensity, capillary diameter, transmission, and the Thompson factor. Scattering from the solvent and empty capillary and electronic noise were subtracted.

3. Results and Their Interpretations

3.1. SEM and TEM Observations: The Chain-like Aggregation. The originally reported method results in the formation of large aggregates of particles.[12] In an attempt to reduce this phenomenon, a number of approaches have been tested, including decreasing of the electrolyte concentration in the surrounding liquid, addition of surfactants and polymers, dilution, and use of smaller TEOS amounts. The most fruitful attempt involved the addition of the lipopolymer mPEG^{2000}-DSPE, which has a poly(ethylene glycol) (PEG) chain. Liposomes to which the lipopolymer had been added have been shown to remain stable in solution because of the protruding PEG strings.[26,27] The hope was to see a similar effect for the liposils. The resulting particles were still aggregated, but the morphology of the aggregates had changed in an intriguing way: unlike the liposil aggregates, where particles fuse to each other in all directions forming 3D clusters, the PEG-liposils tend to form chain-like arrangements. The TEM pictures seen in Figure 1 clearly depict the difference between these two cases. The tendency toward linear aggregation

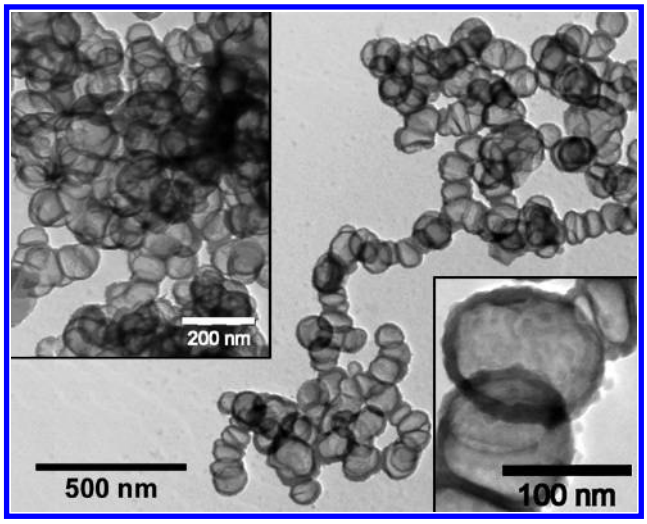

Figure 1. TEM images. Center: A chain-like PEG-liposil aggregate. Upper left: A three-dimensional aggregate of non-PEGilated liposils. Lower right: An enlarged PEG-liposil; note the surface texture.

was seen in HR-SEM micrographs as well (not shown). TEM (Figure 1) and HR-SEM (not shown) images also showed that the surfaces of liposils and PEG-liposils appear to have a rough texture, as if they were covered with granules. Another interesting point arises when looking at the common walls between two adjoining PEG-liposils. The particles seem to be flattened at these sections. In addition, the connecting shells are often thinner than shell parts that are free of contact. Begu et al.[12] suggested that particle fusion takes place while the shell is still in formation. The above observation indicates that this is indeed the case: When two particles are fused, they flatten against each other, so no more silica can reach their contact area, and the connecting wall remains thin. The cryo-TEM analysis, described next, provides further confirmations to these observations and to the suggested mechanism of chain-like aggregate formation.

3.2 Cryo-TEM Observations of the PEG-Liposils Formation Process. Cryo-electron microscopy has proven to be a powerful tool in the study of structures and processes in aqueous environments, which, by this methodology, are vitrified and kept at cryogenic temperatures throughout the analysis. Unlike freezing, where ice crystals are formed, vitrification keeps the water molecules in an amorphous arrangement, close to their liquid state. This preserves nanoaggregates in their original, hydrated state. The low temperature of the sample also helps reduce the damaging effects of the electron beam.[28]

Indeed, we have followed the formation steps of the PEG-liposils, beginning with the liposomes. Figure 2a depicts the DPPC/MPEG-DSPE liposomes. For comparison, the liposomes formed from DPPC only are shown in Figure 2b. It is seen that in denser areas the liposomes are packed together in a honeycomb fashion, unlike the PEG-liposomes, which maintain a distance from each other. This reflects the stabilizing steric effect of the PEG chains, mentioned above. Both samples are evidently faceted. Recall that the phospholipid bilayers exhibit a phase transition upon heating. At a certain point they pass from a paracrystalline or solid state to a fluid condition where rotation occurs around the carbon−carbon bonds of the acyl side chains. For DPPC liposomes, this temperature is 41 °C. The cryo-TEM samples were vitrified from room temperature, which is below this transition point; vesicle faceting is therefore a result of the bilayer rigidity at its solid phase.

(25) Danino, D.; Bernheim-Groswasser, A.; Talmon, Y. *Colloids Surf., A* **2001**, *183*, 113−122.
(26) Torchilin, V. P.; Papisov, M. I. *J. Lipos. Res.* **1994**, *4*, 725−739.
(27) Lasic, D. D. *Nature* **1996**, *380*, 561−562.
(28) Dubochet, J.; Adrian, M.; Chang, J. J.; Homo, J. C.; Lepault, J.; McDowall, A. W.; Schultz, P. *Quart. Rev. Biophys.* **1988**, *21*, 129−228.

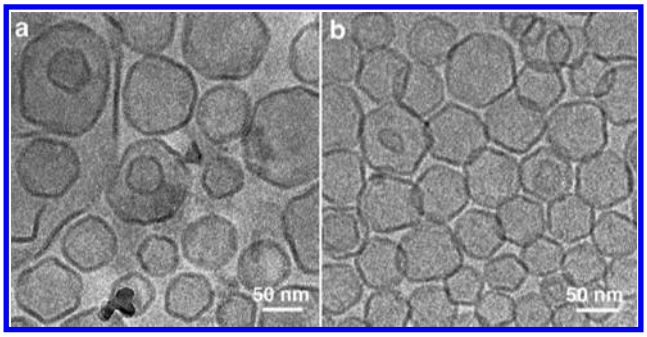

Figure 2. Cryo-TEM images of (a) 1 mg/mL DPPC/MPEG-DSPE liposomes and (b) 10 mg/mL DPPC liposomes.

Figure 3a was taken from a batch of PEG-liposils 11 h into the synthesis. The onset of the sol−gel process induces the formation of large contact areas between the particles (arrow). Presumably, the silica acts as a binding agent, causing them to bond. Assuming that the bilayer is still intact, the tendency toward faceting still exists. The soft vesicles, which are pulled toward each other, "coordinate" their facets under the pressure of adhesion, and in this way large contact areas are formed. Linear aggregates are already visible at this stage.

Figure 3b depicts the sample at 16 h. Aggregates are already well-formed and the particles are rounded. They resemble their final state. Careful inspection of the single PEG-liposil (inset) reveals rough texture on the rim and surface, referred to in the previous section, which is even more evident after 23 h (arrow in Figure 3c). We also observed after 16 h (not shown) and after 23 h (Figure 3c) tiny particles, probably a silica colloid, which is likely to be the source of the textured surface. These colloidal particles settle and fuse on the liposome surfaces. They also seem to fuse to each other in solution, creating a larger colloid, which also settles on the PEG-liposil surface (arrowheads). Alternatively, they may grow on the membranes as well as in solution. The resulting textures can both be seen in Figure 3c. Images of later stages in the synthesis do not reveal any further visible changes (not shown). This sequence of observations reveals then the stage at which aggregation begins, which is quite close to the beginning of the process. This means that the particles are indeed aggregated during formation, not merely stuck to each other at a later stage or while drying the solution. The bilayer crystallinity may play a role in the aggregation process by encouraging shell flattening. The textured surface and presence of silica colloid were also observed in liposil samples, indicating a formation process similar to that of the PEG-liposils.

Why do the PEG-liposils tend toward chain-like aggregation while regular liposils do not? The following facts were used to suggest a mechanism for this unique form of aggregation: (1) mPEG^{2000}-DSPE causes the liposomes to be repelled from each other, probably through steric hindrance, as seen when comparing parts a and b of Figure 2. (2) The aggregation begins quite soon after the addition of the TEOS to the system. (3) The liposomes flatten against each other once aggregation begins. (4) Above the phase transition temperature phospholipids can undergo lateral movement, which allows individual molecules to "float" across the membranes (which maybe possible, but at much slower rate, at lower temperatures). The suggested mechanism is illustrated in Scheme 1: Silica enhances the attraction between two liposil particles, overcoming the steric repulsion caused by the PEG chains. The liposils flatten against each other in the contact zone. The PEG chains are squeezed out of the contact area, due to their bulkiness and mutual repulsion, and move to other parts of the liposome by the lateral motion of their hydrophobic tails across the bilayer. The PEG concentration in the rest of the liposome is increased significantly because of the large contact area between the particles, from which mPEG^{2000}-DSPE is excluded. The concentration may be especially increased around the perimeter of the contact area. The repulsion caused by this larger concentration of PEG is more difficult to overcome, and if a third particle adheres to one of the two fused liposils, the PEG concentration in the central liposome is even further increased, to a point when repulsion is difficult to overcome and a fourth liposome is not likely to approach. This mechanism assumes that lateral motion is possible even below the phase transition temperature, since the presence of TEOS and mPEG^{2000}-DSPE

Scheme 1. Proposed Mechanism of Chain-like Aggregation[a]

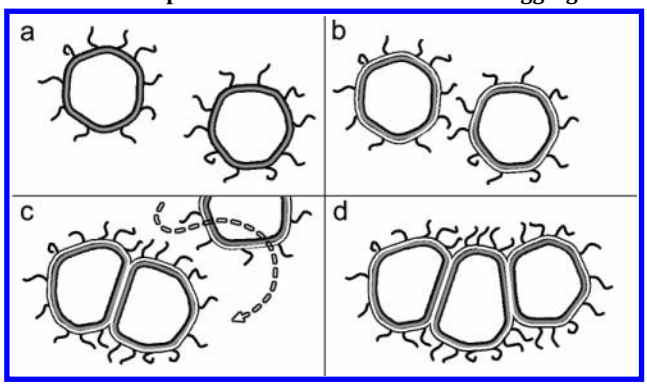

[a] (a) The liposomes are repelled from each other due to the presence of PEG chains. (b) Silica begins to form around the liposomes. (c) The silica enables liposome adherence. As the liposomes bond, they flatten against each other, forcing the PEG chains to slide away from the connecting area and crowd along the sides. When a third particle approaches at this point, it is repelled from the area denser with PEG. It is thus more likely to connect at the farther end of the particle. (d) Once the third liposome is attached, the PEG arrangement on the central liposome becomes even denser. This makes it unlikely for a fourth particle to approach the central liposome and form a branching point.

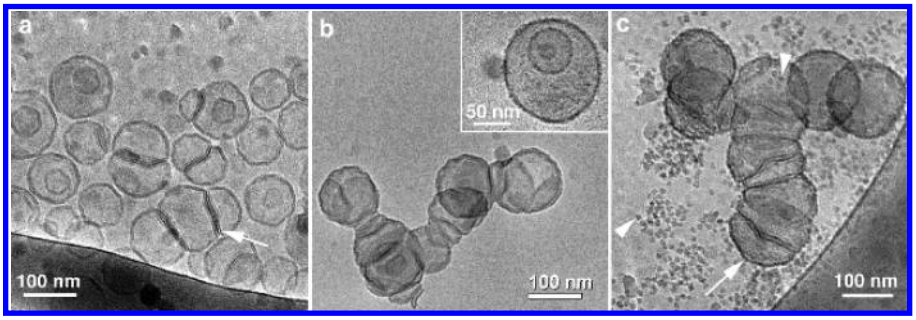

Figure 3. Cryo-TEM images of PEG-liposils. (a) t = 11 h; the arrow points to the fusion domain of two liposils. (b) t = 16 h; the inset shows a liposil decorated with small silica particles. (c) t = 23 h; the arrow points to small silica particles on a liposil membrane and arrowheads point to large silica aggregates.

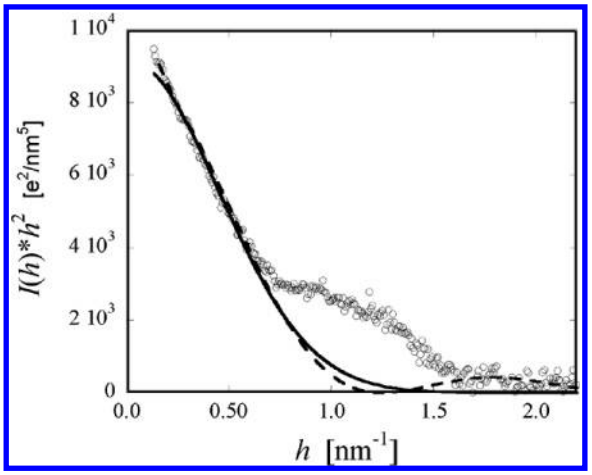

Figure 4. SAXS measurements from the PEG-liposil precipitated from aqueous dispersion (after background subtraction and Lorentz correction). Solid line: fit of the Guinier approximation (eq 1). Dashed line: fit of spherical shell model (eqs 2 and 3).

disturbs the system's crystallinity to some extent. It also assumes that the PEG chains remain exposed and active at least in the early stages of the process. It should be stressed that the lateral motion of the PEG head must occur before the liposome if fully coated by silica.

3.3. SAXS Evaluation of the PEG-Liposil Shell Thickness. Once the overall hollow-shell structure has been established by TEM, a more quantitative evaluation of some characteristic dimensions can be attempted by SAXS measurements. TEM images show that the diameter of the PEG-liposil shells is much larger than the largest dimension probed by the SAXS measurements, estimated as 50 nm ($\sim 2p/h_{min}$, h_{min} being the lowest accessible scattering vector). Thus, structural information on the overall shell structure and its aggregates is beyond this measurement's resolution. We therefore use SAXS to evaluate only information related to the thickness of the particle shell. The scattered intensity from the PEG-liposil in the precipitate of its aqueous dispersion, after normalization and background subtraction, is plotted in Figure 4. It is shown in the Lorentz-corrected form, $h^2I(h)$ vs h, to account for the spread of the intensity in reciprocal space over a spherical shell of radius h, in the geometry of this experiment. Two features are apparent in this scattering pattern: excess scattering at low h, strongly evident even after multiplication by h^2, and a broad shoulder at h of 1.0−1.2 nm^{-1}. The latter appears only after Lorentz correction and thus does not indicate a Bragg reflection due to periodicity.[29] Nevertheless, it suggests the presence of features on the length scale of about 5 nm, which may be some double-layer structures, such as in regions where adjacent shells are flattened and attached to each other (Figure 3), or roughness features of that scale on the shell surface, possibly due to attached small silica particles (Figure 3c). The thickness of the PEG-liposil shell can be evaluated from the low-h scattering. Since the shell diameter is larger than the measurement resolution and the TEM images indicate that many parts of the shell are flattened, we use first the Guinier approximation for a thin flat plate:[30]

$$I(h) \sim \frac{2\pi}{h^2} T^2 e^{-h^2 R_T^2} \quad (1)$$

where T is the layer thickness and R_T is the radius of gyration of the shell cross section, which for a homogeneous density distribution in the cross-section follows $R_T^2 = T^2/12$. The solid line in Figure 4 is a fit of eq 1 to the experimental data, yielding an evaluation of the shell thickness as $T \sim 5.5$ nm. Guinier's approximation is valid for $h < 1/R_T$, which is satisfied in this case, where the fit is for $h < 0.5$ nm^{-1}. To further verify this evaluation of the shell thickness, a model of hollow spherical shells is also used. For a single shell of radius $r = (r_1 + r_2)/2$, defined as the average of the inner (r_1) and outer (r_2) shell radii, and thickness T, the scattering intensity is[31]

$$I_1(h,r,T) = \Delta\rho^2(4\pi/3)^2\{(r + T/2)^3\psi[h(r + T/2)] - (r - T/2)^3\psi[h(r - T/2)]\}^2 \quad (2)$$

where $\Psi(x) = 3(x \cos x - \sin x)/x^3$ is the sphere scattering function and $\Delta\rho$ is the difference in electron density between the shell and its surrounding. For an ensemble of n spherical shells per unit volume, taking into account a Gaussian distribution of sphere radii needed to avoid high-frequency oscillations in the calculated pattern of monodispersed large spheres, the scattering pattern is given by

$$I(h,r,T,\sigma) = n(2\pi)^{-1/2} \int_{r-3\sigma}^{r+3\sigma} I_1(h,r,T) \exp[-(z - r)^2/2\sigma^2]\, dz \quad (3)$$

When fitting this model to the measured data, the only structural parameter to be fitted is the shell thickness T. As mentioned above, the shell diameter is much larger than the resolution of the experimental measurement and thus is not a relevant fit parameter. The sphere radius r is thus arbitrarily set as 50 nm, within the range observed by TEM, with a minimal standard deviation of $s \sim 8$ nm to prevent the oscillations. The dashed line in Figure 4 is the best fit of eqs 2 and 3, providing an average shell thickness of about 5 nm. A good fit is obtained in the low-h region, as with the Guinier approximation. Identical patterns were obtained with any value of the shell radius larger than about 25 nm. The calculated pattern of the spherical shells exhibits a minimum and subsequent maximum in the high-h range, both due to the thickness dimension of the shell. Its position differs distinctly from the broad maximum exhibited in the measured pattern. This supports the analysis made above, whereby the Guinier approximation in the low-h region provides the shell thickness (~5.5 nm) and the broad shoulder at high-h may be due to other small-scale features on the shell surface or the regions of attached shells. Note that the TEM and cryo-TEM pictures reveal varying thicknesses from well below 5 nm up to ~10−12 nm, and thus the SAXS model provides a satisfactory average value.

3.4. ζ-Potential Measurements. PEG-liposils were examined before and after washing with TDW. The mean values of ζ-potential were −40.4 (±3.2) for the unwashed sample and −38.8 (±0.7) for the washed sample, both negative and close to −40 mV. The values are similar, although the solutions are different. The ζ-potential value of a precipitated silica suspension has been reported to be approximately −55 mV at a pH of 7.5 in 2×10^{-2} M NaCl; the suspension was stable at these conditions. Both ζ-potential absolute value and stability of the suspension decreased with increasing electrolyte concentration.[32] The result obtained here for the unwashed solution corresponds reasonably to this report, since the concentration of Na_2HPO_4 that was used in the buffer is 0.013 M and this would release 0.026 M of Na^+

(29) Cser, F. *J. Appl. Polym. Sci.* **2001**, *80*, 358−366.
(30) Porod, G. In *Small-Angle X-ray Scattering*; Glatter, O., Kratky O., Eds.; Academic Press: London, 1982; Chapter 2, p 53.
(31) Glatter, O. In *Small-Angle X-ray Scattering;* Glatter, O., Kratky O., Eds.; Academic Press: London, 1982; Chapter 5, p 181.
(32) Yotsumoto, H.; Yoon, R. H. *J. Colloid Interface Sci.* **1993**, *157*, 434−441.

Scheme 2. Molecular Structures of the Encapsulated Dyes

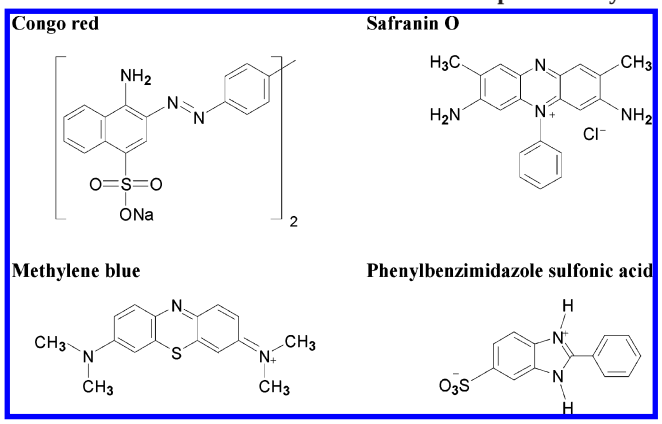

ions. The difference could be attributed to the different electrolytes, to the possible presence of phospholipids in the shell, or to other differences in the silica samples used. The ζ-potential measured for the washed solution is surprising, as it would be expected to be more negative than the value of the unwashed solution, where the electrolyte concentration is higher. Even if the lower pH of TDW, approximately 5−6, is taken into account, the value would be expected to be as low as −70 mV.[33] The similarity between the results could stem from the presence of phospholipids and from the difference in the particle distribution between the two samples, namely, the lack of nanometric silica particles in the washed sample (proven by size distribution analysis, not shown). Another possibility is that the Smoluchowski approximation which was used for the ζ-potential calculations in both cases is less suitable for the washed sample, which has a very low electrolyte concentration.

The results indicate that the PEG-liposils should have been stable in the given conditions, and therefore, aggregation probably occurs at an early stage of the synthesis. This is further supported by the fact that silica displays strong non-DLVO repulsion between surfaces at short distances, probably due to a decrease in the number of hydrogen bonds brought about by the surfaces' close proximity.[32,34] This repulsion increases the stability of silica dispersions.

3.5. Dye Encapsulation in the PEG-Liposils. The dyes, shown in Scheme 2, were encapsulated in the PEG-liposils with the primary goal of using them to identify triggered release. Testing several compounds also helped in assessing the generality of the encapsulation/release technique. The substance that was eventually chosen as a main indicator is Congo Red, which is an anionic water-soluble disazo dye. It has a high absorptivity constant, which was measured in TDW and found to be 43 900 M^{-1} cm^{-1}. The location of its maximum absorbance peak is 497 nm.[35] Safranin O is a cationic water-soluble dye with a maximum absorbance peak at 530 nm in 50% ethanol. Methylene Blue is also a water-soluble cationic dye, it belongs to the thiazines, and has a maximum absorbance at 661 nm in water.[35] Finally, phenylbenzimidazole sulfonic acid is a water-soluble zwitterionic sunscreen agent with an absorbance peak at 303 nm.

The first dye to be tested was CR. The particles formed by using it looked generally normal but did display some degree of inhomogeneity. Samples were washed in water, after which the color did not leach after 2 weeks and longer. PEG-liposil syntheses

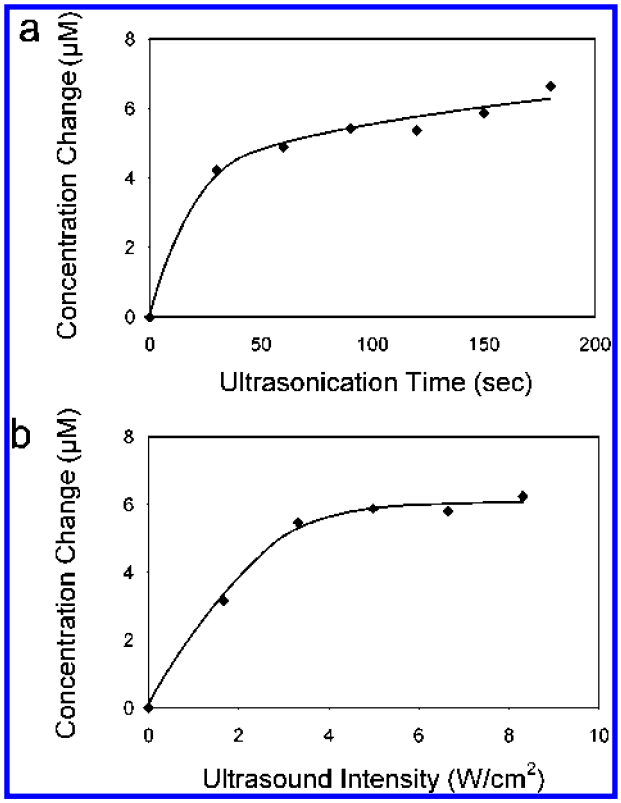

Figure 5. The increase in CR concentration (a) as a function of ultrasonication time, conducted at a constant ultrasonic intensity of 5.0 W/cm^2, and (b) as a function of ultrasound intensity (ultrasonication time = 120 s).

with the other dyes were carried out with the buffer solutions described above. All the syntheses yielded particles. The most homogeneous samples were obtained with MB and PSA. Interestingly, the cationic dyes were adsorbed to the silica and preliminary release results showed low release for these samples. Therefore, the study of these compounds was not continued.

3.6. Variation of the Silica Shell Composition. PEG-liposils containing CR were synthesized with several variations of the silica shell composition to study possible effects of composition on the triggered release properties. The chosen variations included changing the amount of TEOS used, which could affect the shell thickness, and partial substitution of TEOS with the hydrophobic trialkoxysilanes ATMS and OTMS. The latter also opens the option to render the liposils hydrophobic, as may perhaps be needed for various formulations. Particles were obtained in all cases, but some of the samples were less homogeneous and included malformed particles. This mainly includes the ATMS-containing particles and the sample synthesized using one-third of the original TEOS amount.

These examples show that the PEG-liposil silica shell can indeed be modified by the partial substitution of TEOS for other silane monomers. It is important to note, however, that shell modifications have the potential to change not only the particles' endurance to energetic signals but also the degree of encapsulation. Different compositions may produce particles with increased or reduced permeability of the liposil contents, and the number of particles formed successfully in each type may differ, as described above.

3.7. Triggered Release by Ultrasonication. Figure 5 shows a typical profile of the increase in the concentration of released CR from PEG-liposils as a function of US intensity and time (until a low-slope plateau is reached) for sets measured at 120 s and 5.0 W/cm^2, correspondingly. (Error analysis for these

(33) Xu, G.; Zhang, J.; Song, G. *Powder Technol.* **2003**, *134*, 218−222.
(34) Valle-Delgado, J. J.; Molina-Bolivar, J. A.; Galisteo-Gonzalez, F.; Galvez-Ruiz, M. J.; Feiler, A.; Rutland, M. W. *J. Chem. Phys.* **2005**, *123*, Art. No. 034708.
(35) Green, F. J. *The Sigma-Aldrich Handbook of Stains, Dyes and Indicators*; Aldrich Chemical Co.: Milwaukee, WI, 1990.

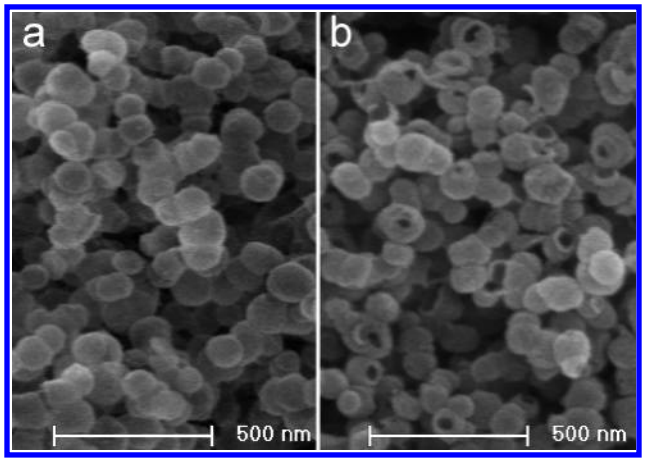

Figure 6. HR-SEM image of PEG-liposils loaded with CR (a) before ultrasonication and (b) after 5 min of ultrasonication at 10 W/cm^2.

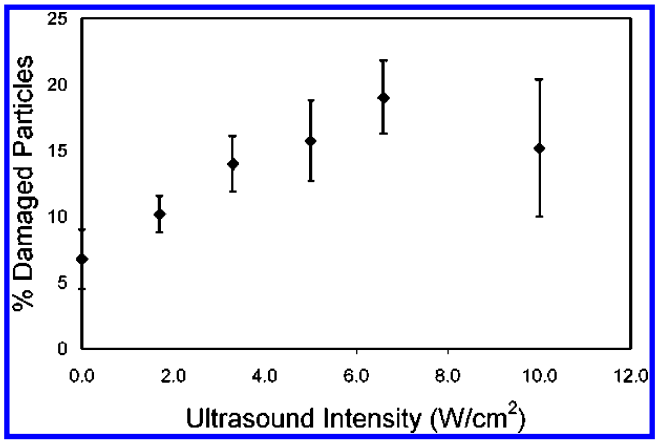

Figure 7. Increase in the percentage of damaged PEG-liposils as a function of ultrasound intensity.

experiments and for the MW experiments is presented below). Perforation of the US-treated particles is clearly evident by comparing parts a (before ultrasonication) and b (after ultrasonication) of Figure 6. A very small portion of the particles is perforated, before being subjected to external energy. Image analysis results for particles that underwent 120 s of ultrasonication at varying intensities are presented in Figure 7.

These results show that the release of dye from the particles upon ultrasonication depends on both time and intensity. That and the increase in the percentage of damaged particles with increasing intensity support the idea that particle rupture is a main mechanism of dye release in the ultrasonication of PEG-liposils. Shell damage that occurs during ultrasonication could be the result of transient cavitation: In a cloud of cavitating bubbles, extreme local pressures and temperatures of up to ~1000 atm and ~5000 K are known to exist, occurring at very rapid heating and cooling rates of 10^{10} K/s,[36] which could cause explosion by steam buildup inside the liposils. Breaking of aggregates could also occur, leaving torn particles at the fracture line. In addition, the shock waves created by cavitation can accelerate solid particles to high velocities and cause collisions,[37] which could shatter the shells and the aggregates. At maximum dye release the percentage of damaged particles is not 100%, and there is not a complete fit between the shape of the release curve

(36) Suslick, K. S.; Didenko, Y.; Fang, M. M.; Hyeon, T.; Kolbeck, K. J.; McNamara, W. B. I.; Mdleleni, M. M.; Wong, M. *Philos. Trans. R. Soc. London, A* **1999**, *357*, 335−353.

(37) Doktycz, S. J.; Suslick, K. S. *Science* **1990**, *247*, 1067−1069.

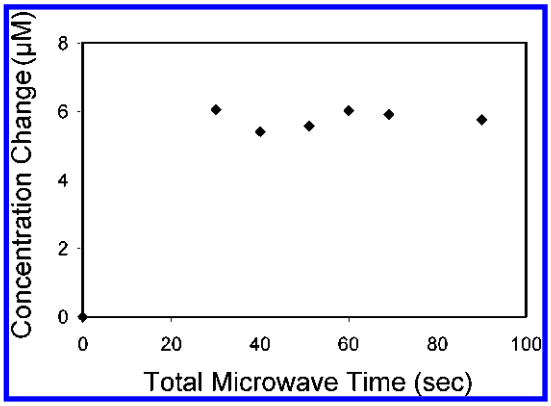

Figure 8. The change in CR concentration as a function of microwave heating time.

Table 1. Typical Errors Calculated for Rupture Experiments on a Single Sample and on Different Samples

instrument	error type	error (%)	instrument	error type	error (%)
microwave	intrabatch	18	ultrasound	intrabatch	16
microwave	interbatch	20	ultrasound	interbatch	15

and the shape of the visual curve. That could be attributed to very small fractures that are not discernible at this magnification (see release by MW below) or to fractures existing on the hidden side of the particle, not visible to the observer. It is in order to mention here briefly previous studies regarding the US-triggered release of drugs from (soft, nonsilicified) liposomes that were shown to follows first-order kinetics with nearly 80% of the drug released within less than 3 min of US irradiation, probably by cavitation near the liposome membrane.[9]

3.8. Triggered Release by Microwave Heating. Microwaving of a set of samples until boiling and then for increasing additional time periods (corresponding to a total radiation time of 30−90 s) gave a set of close results in the range of 5.42−6.05 μM with a mean value of 5.79 μM (Figure 8). The first point, after 30 s, is already the plateau value, indicating the efficiency of that process. Indeed, it should be noted that boiling was already seen in the samples after a few seconds of heating. Longer time of heating, 210 s, caused a decrease in the CR concentration (2.68 μM; not shown). The curve indicates that the triggered release requires a very short heating time: The plateau is reached at the first point of measurement.

Somewhat surprising, the images of the PEG-liposils after typical MW treatment showed significantly less apparent damage compared to images of particles that had undergone ultrasonication. A possible mechanism that explains this is the formation of fissures, smaller than the HR-SEM's resolution, by steam buildup. Such gaps would be sufficient for the passage of dye molecules and would not be visually detectable.

3.9. Error Estimation. The typical error ranges are collected in Table 1.

The results of the error estimations show that the confidence level of quantitatively comparing dye release results of samples from an "average" mixed batch and or from different batches prepared at the same time is 15−20%.

3.10. Effects of Shell Composition Changes on Microwave Triggered Release. Figure 9 collects the release results of CR from capsules of different compositions by MW heating. It is evident that the best encapsulating and release system is that of the 5% ATMS sample. Better rupture due to the incorporation of defects in the form of a foreign alkoxide, or the formation of more particles, or reduction in the amount adsorbed on the silica shell could all account for that observation. Interestingly the 5%

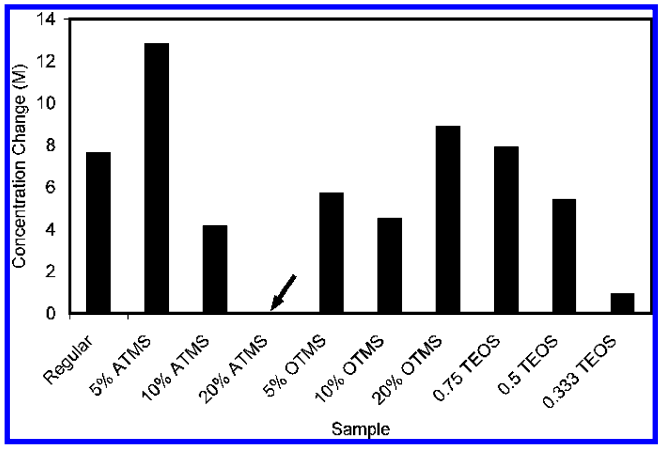

Figure 9. The change in CR concentration for samples with different shell compositions after microwave treatment. The arrow points to an insignificant change in concentration obtained for a 20% ATMS shell.

is an optimal composition; the values drop sharply for 10 and 20%. No special trend is visible for the OTMS samples. As for the reduced amount of TEOS, if the total amount of color trapped in the different samples may be different due to sample defects, the results of dye release experiments cannot be treated as quantitative. This is probably the explanation to the reduction of CR concentration as the amount of TEOS is reduced to one-half and one-third of the original amount.

4. Conclusion

The combination of PEG-liposils with low-frequency US or MW proved to have potential as triggered release systems for aqueous solutions of functional molecules. The suggested mechanism of MW release involves the formation of subnanometric pores by the boiling water core, whereas the mechanisms of release by US are most likely particle rupture and breakage alongside the formation of subnanometric fissures. PEG-liposils were shown here to be suitable carriers for anionic and zwitterionic chemicals, but of course, hydrophilic drugs are an obvious next stage. Shells with various compositions can be formed by the method presented here. The process of particle formation was elucidated by cryo-TEM experiments, which revealed the early formation of aggregates and the involvement of a silica colloid in the shell formation. These experiments also helped suggest a mechanism for chain-like aggregation of PEG-liposil capsules, according to which concentration and lateral movement of the PEG chains across the liposomes are important factors in this formation process. Further applications of the PEG-liposils are under development.

Acknowledgment. Many thanks are due to the European NEO FAME program for promoting this collaborative program. Thanks are also extended to Evgenia Blayvas and the staff of the Unit for Nanocharacterization at the Hebrew University of Jerusalem, to Avi Willenz at the Life-Science Electron Microscopy Unit, to Prof. H. Gilon for putting a MW oven at our disposal, to Prof. S. Magdassi for help and advice, to Prof. Y. Baraneloz for enabling production of liposomes in his lab and for the gift of mPEG-DSPE, and to Prof. J. Kost for providing the US machine used in this work. The cryo-TEM work was performed at the Hannah and George Krumholz Laboratory for Advanced Microscopy, part of the Technion Project on Complex Fluids, Microstructure and Macromolecules. The research was supported by the MAGNET-NFM program of The Israel Ministry for Commerce and Industry.

LA702311F